International Journal of Thermophysics, Vol. 15, No. 6, 1994

Thermophysical Properties of Liquid Iron[1]

M. Beutl,[2] G. Pottlacher,[2,3] and H. Jäger[2]

Wire-shaped iron samples are resistively volume heated as part of a fast capacitor discharge apparatus. Measurements of current through the specimen, voltage across the specimen, radiance temperature, and thermal expansion of the specimen as functions of time allow the determination of specific heat and various dependencies among enthalpy, electrical resistivity, temperature, and density for liquid iron up to 5000 K. High pressures, up to 3800 bar, are used to obtain the liquid state far above the normal boiling point. An estimate of critical-point data for iron is given by using experimental data of the vapor pressure of liquid iron.

KEY WORDS: critical point; electrical resistivity; enthalpy; high pressure; high temperature; iron; liquid metals; melting; specific heat; vapor pressure.

1. INTRODUCTION

There are few data for critical point parameters of metals available, because for most metals they can be deduced only from theoretical models. Therefore, we have continued our work on thermophysical properties of ferromagnetic metals by studying iron in the liquid phase, including an estimation of critical point parameters of iron [1]. Some thermophysical properties of iron have already been measured [2] using a different discharge circuit and a pyrometer which could not resolve the melting plateau of iron. In this earlier paper, thermal expansion was measured only at pressures of 1 bar. As discussed in Ref. 7, therefore, too-high values of sample volume have been measured for higher

---

[1] Paper presented at the Twelfth Symposium on Thermophysical Properties, June 19–24, 1994, Boulder, Colorado, U.S.A.

[2] Institut für Experimentalphysik, Technische Universität Graz, Petersgasse 16, A-8010 Graz, Austria

[3] To whom correspondence should be addressed.

temperature values. For liquid iron, only limited data are available in the literature [3–5].

In the present work, a fast pulse-heating technique was used to reach temperatures far above the melting point of iron ($T_m = 1808$ K [6]). From measurements of current, voltage, temperature, and thermal expansion, the following thermophysical properties are obtained: enthalpy, heat of fusion, specific heat at constant pressure, density, and electrical resistivity in a temperature range from melting up to about 5000 K. Critical point parameters of iron are estimated using experimental data of the vapor pressure of iron.

2. MEASUREMENTS

The iron samples are resistively volume heated far into the liquid phase by passing large current pulses through them. Using two different discharge circuits, heating rates of 10^8 and 10^9 $K \cdot s^{-1}$ were achieved. Wire-shaped iron samples were of 99.99+ purity (Goodfellow Metals, Cambridge, UK), with a typical length of 40 mm and different diameters (0.5 and 0.25 mm). The measurements were conducted in a pressure vessel under static ambient pressures from atmospheric pressure up to 3800 bar to permit nearly isobaric conditions. The pressurizing medium was water.

The discharge circuits consist of capacitors for energy storage (capacitor banks with 500 or 5.4 μF), a fast-acting main switch, and a high-pressure experiment chamber with sapphire windows. A crowbar switch allows one to stop the experiment at any prechosen time. For optical diagnostics, different pyrometers and a new fast-acting CCD camera with an image converting system were used [8].

Time-resolved measured quantities are current through the sample, voltage drop along the sample, surface radiation intensity, and sample radius. The sample radius is measured with a CCD camera, which takes a picture of the diameter of a small part of the sample every 9 μs. These pictures can be processed with the help of an image converting system. The same measurements also demonstrate stability of the specimen during the time of the experiment (about 55 μs). The data were recorded by fast digital oscilloscopes placed in a shielded room and, afterward, processed by a personal computer. Thus, data for enthalpy, temperature, electrical resistivity, and density as functions of time are obtained. For more details one may see Ref. 9. By comparing values at common times, the interdependencies of enthalpy, resistivity, temperature, and volume expansion can be obtained.

3. RESULTS

The data obtained for enthalpy, temperature, electrical resistivity, and volume are presented in form of least-squares fits.

Figure 1 shows a plot of enthalphy versus temperature. The least-squares fit to these data for the range $1808 < T < 5000$ K is given by

$$H = -0.18626 + 8.2516 \times 10^{-4} T \qquad (1)$$

where H is in $\mathrm{MJ \cdot kg^{-1}}$. For the specific heat at constant pressure in the liquid phase a value of $825\ \mathrm{J \cdot kg^{-1} \cdot K^{-1}}$ is obtained, which is in very good agreement with values given in Refs. 3 ($824\ \mathrm{J \cdot kg^{-1} \cdot K^{-1}}$) and 5 ($815.4\ \mathrm{J \cdot kg^{-1} \cdot K^{-1}}$).

Figure 2 shows the density ρ derived from our value for volume against enthalpy. Also shown are values from Ref. 10; temperature values are converted to enthalpy values with the specific heat obtained in this work. The least-squares fit to our data for $1.3 < H < 2.2\ \mathrm{MJ \cdot kg^{-1}}$ is

$$\rho = 8312 - 997H \qquad (2)$$

where ρ is in $\mathrm{kg \cdot m^{-3}}$.

The measured data for volume allow to correct the data on electrical resistivity due to thermal expansion. The electrical resistivity without thermal expansion ($\rho_{\mathrm{el},0}$; dashed line) and the volume corrected values

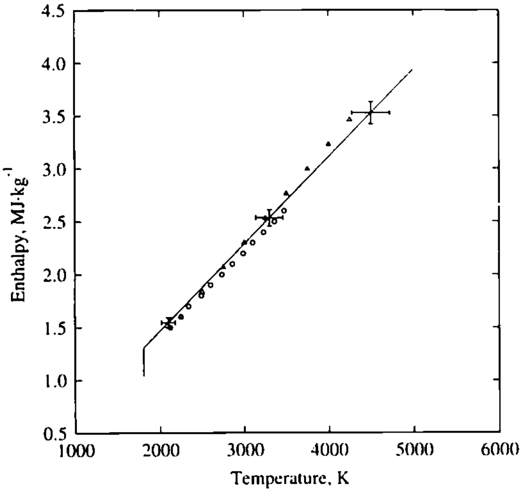

Fig. 1. Variation of enthalpy as a function of temperature for iron. Solid line, this work; triangles, data from Ref. 10; circles, data from Ref. 5.

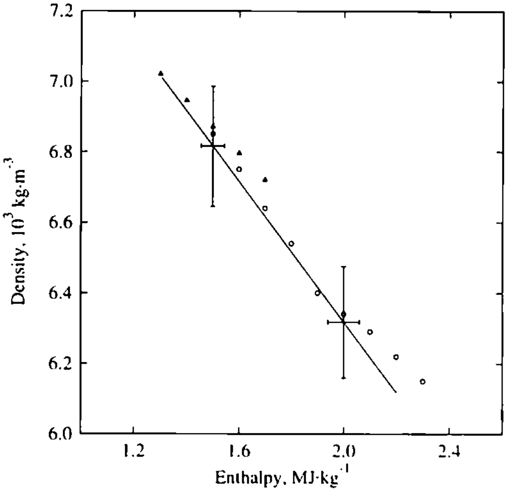

Fig. 2. Variation of density as a function of enthalpy for iron. Solid line, this work; triangles, data from Ref. 10; circles, data from Ref. 5.

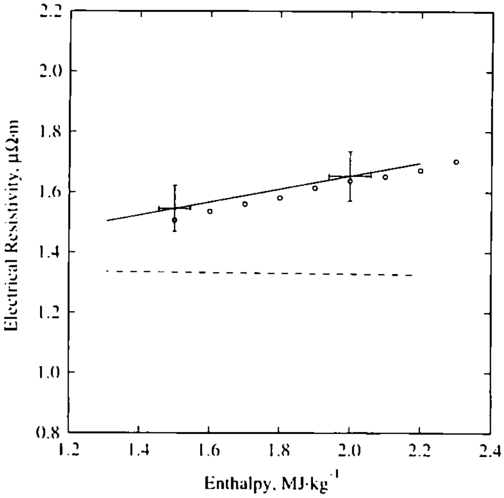

Fig. 3. Variation of electrical resistivity as a function of enthalpy. Electrical resistivity without thermal expansion, dashed line; volume-corrected values, solid line; data from Ref. 5, circles.

(ρ_{el}; full line) plotted against enthalpy are shown in Fig. 3. The least-squares fit to the data of the uncorrected electrical resistivity in the range of $1.3 < H < 2.2\ \mathrm{MJ \cdot kg^{-1}}$ at a pressure of 2000 bar is given by

$$\rho_{\mathrm{el},0} = 1.360 - 0.013H \tag{3}$$

where $\rho_{\mathrm{el},0}$ is in $\mu\Omega \cdot \mathrm{m}$. The corrected electrical resistivity within this range is given by

$$\rho_{\mathrm{el}} = 1.221 + 0.216H \tag{4}$$

The values agree with the data in Ref. 5 within our uncertainties.

Our obtained values for specific heat for the liquid phase, melting enthalpy, enthalpy and electrical resistivity at the beginning and at the end of melting, compared with literature data, are given in Table I. Experimental results on the properties obtained in the present work are given in Table II.

Critical-point data can be estimated by the following considerations, which are discussed in detail in Ref. 1: The temperature values reach a maximum while the enthalpy values are still increasing. For higher static pressures this maximum turns to higher temperatures. The reason for the temperature decreasing after reaching a maximum value could be distortions of the radiating surface, which are due to boiling, when reaching the spinodal line at the given pressure.

A vapor pressure equation can be derived from the Clausius–Clapeyron equation by assuming an ideal behavior of the gas, neglecting the specific volume of the liquid compared with the gas, and a heat of vaporization, which is independent of temperature:

$$\ln p_{\mathrm{v}} = A + B/T \tag{5}$$

Table I. Thermophysical Properties of Iron: Enthalpy at the Beginning, H_{S}, and End, H_{L}, of the Melting Phase Transition, Melting Enthalpy, ΔH, Electrical Resistivity at the Beginning, ρ_{S}, and End of Melting, ρ_{L}, and Specific Heat, c_{p}, for the Liquid Phase, Compared with the Values of Other Investigators

Investigators	Ref. No.	H_{S} ($\mathrm{MJ \cdot kg^{-1}}$)	H_{L} ($\mathrm{MJ \cdot kg^{-1}}$)	ΔH ($\mathrm{MJ \cdot kg^{-1}}$)	ρ_{S} ($\mu\Omega \cdot \mathrm{m}$)	ρ_{L} ($\mu\Omega \cdot \mathrm{m}$)	c_{p} ($\mathrm{J \cdot kg^{-1} \cdot K^{-1}}$)
This work		1.040	1.306	0.265	1.42	1.50	825
Hultgren et al.	3	1.050	1.297	0.247			824
Pottlacher et al.	2	1.061	1.330	0.269	1.29	1.36	
Seydel et al.	4	1.051	1.328	0.277			
Hixson et al.	5						815.4

Table II. Experimental Results on the Thermophysical Properties of Iron Obtained in this Work: Enthalpy, H; Temperature, T; Density, ρ; and Electrical Resistivity, $\rho_{\mathrm{el,0}}$ and ρ_{el} (Without and with Correction for Thermal Expansion)

H $(\mathrm{MJ \cdot kg^{-1}})$	T (K)	$\rho_{\mathrm{el,0}}$ $(\mu\Omega \cdot \mathrm{m})$	ρ_{el} $(\mu\Omega \cdot \mathrm{m})$	ρ $(\mathrm{kg \cdot m^{-3}})$
$1.04^{(s)}$	1808	$1.29^{(s)}$	$1.42^{(s)}$	
$1.31^{(l)}$	1808	$1.34^{(l)}$	$1.50^{(l)}$	$7010^{(l)}$
1.50	2044	1.34	1.55	6817
1.75	2347	1.34	1.60	6567
2.00	2649	1.33	1.65	6318
2.25	2952	1.33	1.71	6069
2.50	3255			
2.75	3558			
3.00	3861			
3.25	4164			
3.50	4467			
3.75	4770			

where p_v is the vapor pressure and A and B are constants. Equation (5) cannot be used for an extrapolation up to the critical point, because the heat of vaporization decreases with increasing temperature and vanishes at the critical point. Besides, the assumptions of ideal-gas behavior and negligibly small volume of the liquid cannot be sustained any longer.

If the temperature dependence of the heat of vaporization is considered to be of the form

$$\Delta H_V - \Delta H_{V,0} = \int_0^T \left(c_p^{(g)} - c_p^{(l)}\right) dT' \qquad (6)$$

where ΔH_V is the extrapolation to $T = 0$ K and $c_p^{(g)}$ and $c_p^{(l)}$ are the heat capacities at constant pressure in the gas and in the liquid, respectively, and assuming $\Delta c_p = c_p^{(g)} - c_p^{(l)}$ to be independent of temperature, one obtains the following equation:

$$\ln p_v = A' + B'/T + C' \ln T \qquad (7)$$

with A', B', and C' being constants. Although Δc_p should also vanish at the critical point, in some cases such a three-term equation fits the experimental data up to the critical point quite well [11].

Vapor pressure data for iron from room temperature up to the boiling point at atmospheric pressure have been given in Ref. 3. Using Eq. (7) we

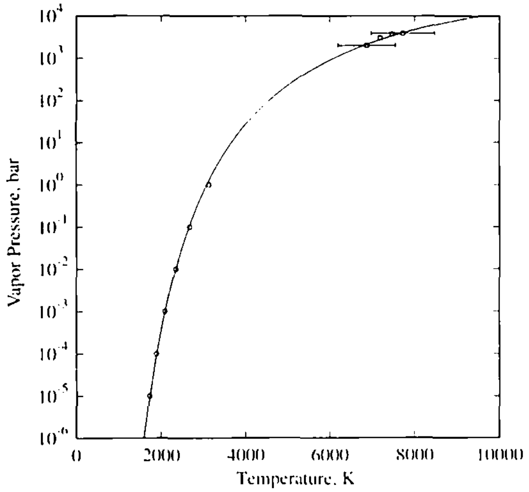

Fig. 4. Vapor pressure versus temperature for iron. Circles, data at atmospheric pressure from Ref. 3; squares, data points measured in this work (uncertainty is indicated).

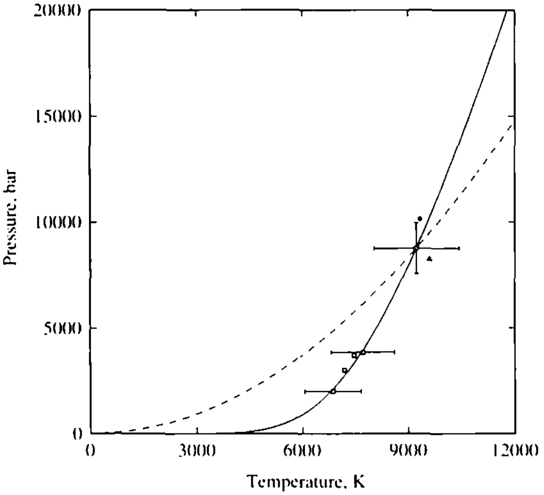

Fig. 5. Intersection of Eq. (9) (Likalter relation; dashed line) with the experimentally obtained vapor pressure curve (solid line). Open squares, data points measured in this work; full triangle, critical point data from Ref. 16; full square, critical point data from Ref. 14.

Table III. Obtained Values for the Critical Pressure, p_c, and the Critical Temperature, T_c, Compared with Data of Other Investigators

Investigators	Ref. No.	T_c (K)	p_c (bar)
This work		9,250 ± 12%	8,750 ± 14%
Fortov et al.	14	9,600	8,250
Hornung	15		10,291.8
Young and Alder	16	9,340	10,154
Kopp	17	9,400	

tried to fit our data at high pressures and the data from Ref. 3, which leads to the following constants:

$$A = 26.4317, \qquad B = -48769\text{ K}, \qquad C = -1.3217 \tag{8}$$

with a mean square error of 0.056 for the fitted polynomial corresponding to an uncertainty of about ±14% in the pressure. Figure 4 shows the obtained curve for the vapor pressure of iron.

Under the assumption that Coulomb interaction dominates the attractive forces in a liquid metal around its critical point, Ref. 12 suggested a procedure to estimate critical data using a relation between the critical pressure and the critical temperature given in Ref. 13, which tries to adapt the van der Waals equation to the conditions in a liquid metal near its critical point. The actual critical point value for iron is obtained in Fig. 5 from the point of intersection of Eq. (9) (dashed line in Fig. 5) with the experimentally obtained vapor pressure curve (solid line in Fig. 5).

It could be shown for the alkali metals [12] that the Likalter relation takes the following form:

$$p = (1.66 \pm 0.12)\, 10^{-6} (TE_i)^2 \tag{9}$$

where p is the pressure in bar, T is the temperature in K, and E_i is the ionization energy of the undisturbed atom ($E_i = 7.87$ eV). The obtained critical-point data are compared in Table III with those of other investigators.

4. ESTIMATION OF ERRORS

Enthalpy is the most accurate of all the properties measured, with an estimated uncertainty of ±3%. For temperature measurements the uncertainty is ±3% in the melting region, increasing to about ±12% at the critical point. The error in the uncorrected electrical resistivity is estimated to be ±3%, increasing to ±6% for the corrected electrical resistivity. An error of ±3% is estimated for the density. The estimated uncertainty in the value of melting enthalpy is 5%; that in the value of specific heat is ±7%. The error in the vapor pressure values is estimated to be ±14%.

5. CONCLUSIONS

The thermophysical properties of liquid iron were investigated by using a fast pulse-heating technique. The mutual dependencies among enthalpy, temperature, density, and electrical resistivity have been obtained, as well as the melting enthalpy and the specific heat, and they are in good agreement with the results of other authors. In addition, some vapor pressure data have been obtained at higher pressures by interpreting the maximum in the temperature traces while the enthalpy increases further as the start of vaporization. Combining the obtained vapor pressure equation with a relation between the critical pressure and the critical temperature [12], we estimated critical-point values of temperature and pressure for iron.

REFERENCES

1. H. Hess, E. Kaschnitz, and G. Pottlacher, *High Press. Res.* **12**:29 (1994).
2. G. Pottlacher, H. Jäger, and T. Neger, *High Temp. High Press.* **19**:19 (1987).
3. R. Hultgren, P. D. Desai, D. T. Hawkins, M. Gleiser, K. K. Kelley, and D. D. Wagman, *Selected Values of Thermodynamic Properties of the Elements* (ASM, Metals Park, OH, 1973).
4. U. Seydel, H. Bauhof, W. Fucke, and H. Wadle, *High Temp. High Press.* **11**:35 (1979).
5. R. S. Hixson, M. A. Winkler, and M. L. Hodgdon, *Phys. Rev. B* **42**:6485 (1990).
6. A. Cezairliyan and J. L. McClure, *J. Res. Natl. Bur. Stand.* **79A**:541 (1975).
7. H. Jäger, W. Neff, and G. Pottlacher, *Int. J. Thermophys.* **13**:83 (1992).
8. G. Nussbaumer, Diploma thesis (Technische Universität Graz, Graz, 1993).
9. E. Kaschnitz, G. Nussbaumer, G. Pottlacher, and H. Jäger, *Int. J. Thermophys.* **14**:251 (1993).
10. W. D. Drotning, *High Temp. High Press.* **13**:441 (1981).
11. J. Magill and R. W. Ohse, in *Handbook of Thermodynamic and Transport Properties of Alkali Metals*, R. W. Ohse, ed. (Blackwell Scientific, Oxford, 1985), p. 73.
12. H. Hess, in *Physics of Nonideal Plasma*, W. Ebeling, A. Förster, and R. Radtke, eds. (B. G. Teubner Verlagsgesellschaft, Stuttgart, Leipzig, 1992), p. 131.
13. A. A. Likalter, *Teplofiz. Vys. Temp.* **23**:465 (1985).
14. V. E. Fortov, A. N. Dremin, and A. A. Leontyev, *Teplofiz. Vys. Temp.* **13**:172 (1975).
15. K. Hornung, *J. Appl. Phys.* **46**:2548 (1975).
16. D.A. Young and B. J. Alder, *Phys. Rev. A* 3:364 (1971).
17. I. Z. Kopp, *Zh. Fiz. Khim.* **41**:1474 (1967).